HHS Public Access

Author manuscript

Biomaterials. Author manuscript; available in PMC 2024 August 21.

Published in final edited form as:

Biomaterials. 2024 April ; 306: 122494. doi:10.1016/j.biomaterials.2024.122494.

A hybrid nanoparticle-protein hydrogel system for prolonged local anesthesia

Wonmin Choi,

Gil Aizik,

Claire A. Ostertag-Hill,

Daniel S. Kohane*

Laboratory for Biomaterials and Drug Delivery, Department of Anesthesiology, Division of Critical Care Medicine, Boston Children's Hospital, Harvard Medical School, 300 Longwood Avenue, Boston, MA, 02115, United States

Abstract

Local anesthetics are effective in relieving pain, but their duration of action is short. Therefore, the development of injectable sustained release systems to prolong the effect of local anesthetics has been of interest. In such systems delivering conventional local anesthetics, it has been challenging to achieve long durations of effect, particularly without incurring tissue toxicity. To overcome these challenges, we created a platform comprising a protein hydrogel incorporating hydrophobic local anesthetic (bupivacaine) nanoparticles. The nanoparticles were prepared by anti-solvent precipitation stabilized with bovine serum albumin (BSA), followed by cross-linking with glutaraldehyde (GA). The resulting BSA hydrogels prolonged release of bupivacaine *in vitro*. When bupivacaine nanoparticles within crosslinked BSA were injected at the sciatic nerve in rats, a duration of nerve block of 39.9 h was obtained, compared to 5.5 h for the commercial bupivacaine liposome suspension EXPAREL®. Tissue reaction was benign. We further demonstrated that this system could control the release of the amphiphilic drug diphenhydramine and the hydrophobic paclitaxel.

Keywords

Protein hydrogel; Drug nanoparticle; Crosslinking; Nerve block; Local anesthesia

*Corresponding author. daniel.kohane@childrens.harvard.edu (D.S. Kohane).

CRediT authorship contribution statement

Wonmin Choi: Writing – review & editing, Writing – original draft, Formal analysis, Data curation, Conceptualization. **Gil Aizik:** Formal analysis, Data curation. **Claire A. Ostertag-Hill:** Formal analysis, Data curation. **Daniel S. Kohane:** Writing – review & editing, Supervision, Project administration, Conceptualization.

Declaration of competing interest

The authors declare that they have no known competing financial interests or personal relationships that could have appeared to influence the work reported in this paper.

Appendix A. Supplementary data

Supplementary data to this article can be found online at https://doi.org/10.1016/j.biomaterials.2024.122494.

1. Introduction

Local anesthetics are extremely effective at preventing the perception of pain when injected at a painful body location, or at a nerve leading to the site. However, one shortcoming is their relatively short duration of effect [1]. For decades, investigators have been developing injectable sustained release systems to prolong that duration, investigating a wide range of vehicles [2–4]. Initial interest was driven by the desire to alleviate pain and suffering, and to prevent physiological derangements associated with it. Since the advent of the opioid epidemic, interest in prolonged local anesthesia (PLA) has also been driven by the potential to replace opioids in the treatment of relatively localized pain (e.g., after shoulder surgery [5,6]) for the duration of the perioperative period (a few days).

The effect of conventional local anesthetics delivered by injectable PLA systems is typically several fold, but – in the absence of adjunctive drugs such as glucocorticoid steroids – they rarely achieve even a day of nerve block in established models [7]. As one example, in our animal model, the commercially available liposomal bupivacaine formulation EXPAREL® only provides 4–8 h of nerve block [8]. One important limitation in this regard is that conventional local anesthetics are relatively low in potency, which limits the effectiveness of the payload [9,10].

Here we developed a hybrid nanoparticle-hydrogel approach to extending the effect of conventional local anesthetics, using the commonly used agent bupivacaine as an example. We self-assembled bupivacaine in the hydrophobic free base form into nanoparticles, to maximize loading and slow release. The bupivacaine nanoparticles were formed in the presence of bovine serum albumin (BSA) to enhance nanoparticle stability [11] and prevent aggregation [12–14]. Since BSA also binds hydrophobic drugs such as bupivacaine, it could also slow release. Moreover, BSA can be cross-linked to create a macroscopic hydrogel [15], further slowing the release of bupivacaine, and maintaining the nanoparticles at the site of administration. We demonstrated that this approach could be generalized by showing that different drugs (diphenhydramine and paclitaxel) incorporated into the platform had slowed release compared to free drugs.

The increased loading and slowed release that could be achieved by nanoparticles of carrier-free hydrophobic bupivacaine in a cross-linked albumin matrix could lead to extended nerve block. Equally importantly, the reduction in release rate could mitigate the severity of local tissue injury. Local anesthetics can cause inflammation at the site of injection, as well as injury to muscle and nerve. These toxicities can be worsened by sustained release, in a manner dependent on the level and duration of release. This toxicity can limit the duration of effect of systems releasing conventional local anesthetics.

2. Results

2.1. Synthesis and characterization of BNP@BSA-X

A glutaraldehyde-crosslinked bovine serum albumin hydrogel (BSA-X) containing bupivacaine free base nanoparticles (BNPs), abbreviated BNP@BSA-X, was made by a one-pot approach (Scheme 1). In brief (see Methods) the free base of the amphiphilic drug

bupivacaine was produced by alkaline precipitation of bupivacaine hydrochloride. The free base was then dissolved in methanol and introduced dropwise into bovine serum albumin (BSA) in phosphate-buffered saline (PBS) at pH 7.4, yielding bupivacaine nanoparticles within BSA (BNP@BSA). The methanol was evaporated by rotary evaporation. Finally, glutaraldehyde (GA) was added to crosslink the BSA and form a BSA hydrogel with embedded BNPs (BNP@BSA-X).

The hydrodynamic diameter of BNPs in BSA prior to crosslinking was ~190 nm by dynamic light scattering (DLS) (Fig. 1A), with a narrow size distribution. There was also a population of ~7 nm NPs, corresponding to BSA protein [16]. After washing to remove excess BSA [11,17], BNP@BSA measured 70–100 nm by transmission electron microscopy (TEM; Fig. 1B). The discrepancy between diameters by TEM and DLS is because the latter measures the hydrodynamic diameter [18].

While the interaction between bupivacaine and serum albumin has been extensively studied [19–23], the interaction between BNP and serum albumin has not been reported. We investigated the interaction between BNP and BSA by measuring their fluorescence and UV–Vis spectra (Fig. 1C and Figure S1 in Supporting Information) [24–27]. Upon adding BNP (0.05, 0.1, and 0.2 mg/ml) to the BSA solution (1 mg/ml), there was quenching of the emission peak of BSA at around 335 nm upon excitation at 280 nm (Fig. 1C). This peak is associated with the intrinsic fluorescence of tryptophan residues in BSA. The observed quenching suggests potential molecular interactions, possibly induced by energy transfer or molecular rearrangement of BSA [24–30]. BNP alone in PBS did not show any emission in this wavelength range upon the same excitation, indicating that these changes in spectra are related to BSA.

UV–Vis absorption studies revealed a shift in the spectra of BSA around 260 nm with introduction of BNP (Figure S1 in Supporting Information). This shift can be attributed to the $\pi \rightarrow \pi^*$ transition of aromatic amino acids, including Trp, Tyr, and Phe in BSA [30–32]. Additionally, alterations in the spectra of BSA in the 210–230 nm range indicated changes in the structural conformation of BSA following the addition of BNP [30–32]. The BNP alone in PBS did not show distinct absorbance in this range of wavelengths, demonstrating that these absorbance changes are related to structural changes in BSA.

BNP@BSA-X was synthesized using 50 mg/ml or 100 mg/ml of BSA and 5 mg/ml or 10 mg/ml of GA. In contrast to BNP in PBS and BNP@BSA, which did not form hydrogels, all BNP@BSA-X samples formed hydrogels (Figure S2 in Supporting Information). In all hydrogel samples, gelation occurred in ~1 s. Residual glutaraldehyde was not detected by high-performance liquid chromatography (HPLC) after the 24 h incubation of BNP@BSA-X in PBS (Figure S3 in Supporting Information; see method) [33].

The BNP@BSA-X hydrogels had a storage modulus (G') greater than the loss modulus (G'') at all concentrations of BSA and GA, indicating solid-like properties (Figure S4 in Supporting Information). 10 mg/ml GA resulted in a higher G' (e.g., at 10^2 rad/s angular frequency) than 5 mg/ml GA with BSA at 50 mg/ml ($p = 0.045$) and 100 mg/ml ($p = 0.021$), likely due to increased crosslinking between BSA proteins (Fig. 1D and Figure S4 in

Supporting Information). Since all the BNP@BSA-X formed hydrogels, we used those with 50 mg/ml BSA (with 5 or 10 mg/ml of GA) in downstream experiments, to minimize the mass to be injected *in vivo*.

Here, drug nanoparticles are contained within a cross-linked albumin hydrogel. Cross-linking would occur prior to administration a) to ensure that the cross-linking occurs within the drug delivery system rather than with tissues, b) to minimize the extent to which the system will dissipate after injection, c) to reduce the need for rapid cross-linking *in vivo*. For this purpose, it would be desirable to have shear-thinning properties, i.e., for the material to be highly elastic prior to injection, be readily injectable, then to regain elasticity after injection [34]. We evaluated the mechanical properties of BNP@BSA-X formulations by rheometry through step-strain oscillations (Fig. 1E and Figure S5 in Supporting Information). For BNP@BSA-X (5 mg/ml GA), the application of high strain (500 %) led to liquid-like properties, with G' < G" (Fig. 1E). Upon the removal of excess strain (to 0.1 %), G′ exceeded G″ within seconds. Over repeated cycles, near-complete healing was achieved. BNP@BSA-X (10 mg/ml GA) exhibited a decrease in G′ with repeated strain cycles at 0.1 % (Figure S5 in Supporting Information). When exposed to high strain, G′ closely approached G″, suggesting a lack of shear-thinning behavior. BNP@BSA with 10 mg/ml GA was hard to inject through a 23-gauge needle. BNP@BSA-X with 50 mg/ml BSA and 5 mg/ml GA was used in downstream studies.

Scanning electron microscopy of BNP@BSA-X showed a pore size of approximately 5–10 μm, suggesting a large surface area and high water-absorption capacity (Figure S6 in Supporting Information).

The release of bupivacaine from BSA formulations containing bupivacaine•HCl was similar to that of bupivacaine•HCl alone (for the comparison of the latter to bupivacaine•HCl@BSA at 24h, p = 0.18; to bupivacaine•HCl@BSA-X; p = 0.54)(Fig. 1F). In contrast, the release of bupivacaine from BNP (formed in the absence of albumin) was slower than from bupivacaine•HCl (p = 0.0005 at 24 h). The hydrophobic nature of the free base, and the particulate nature of BNP could have contributed to the slower release. These findings highlight the importance of nanoparticle formation in achieving sustained release.

Bupivacaine release from BNP@BSA and BNP@BSA-X was much slower than from BNP in PBS (both $p < 0.0001$ at 24 h), underscoring the significant role of BSA in slowing release.

The release kinetics of BNP@BSA and BNP@BSA-X were similar (p = 0.085 at 24 h). This similarity *in vitro* could be due the fact that the dialysis device physically constrained the BSA solution within a fixed volume at the same concentration as BSA-X, i.e., mimicking a cross-linked hydrogel.

2.2. Release of other compounds

To illustrate the broader applicability of this approach to different drugs, we used diphenhydramine, an antihistamine, as an example of another amphiphilic drug (water solubility: 683 mg/ml for the hydrochloride salt form [35], log P: 3.50 for the free base form

[36]), and paclitaxel, a hydrophobic chemotherapy drug (water solubility <0.1 μg/ml, log P: 3.20 [37]) (Fig. 2 and Figure S7 in Supporting Information). Nanoparticles were prepared from both drugs and incorporated into crosslinked BSA. In brief, the free base form of diphenhydramine was generated by adding triethylamine (TEA) to diphenhydramine•HCl in methanol then added dropwise to a 50 mg/ml BSA solution in pH 7.4 PBS. After evaporating the methanol, glutaraldehyde (GA) was added to crosslink the BSA, forming diphenhydramine nanoparticles in cross-linked BSA (DHNP@BSA-X). Paclitaxel was dissolved in methanol and added to a 50 mg/ml BSA solution in pH 7.4 PBS. Methanol was evaporated, then GA was added to create paclitaxel nanoparticles in cross-linked BSA (PNP@BSA-X). The diameter of DHNP (~10–30 nm) and PNP (~10–20 nm) before crosslinking was verified by TEM (Figure S7B in Supporting Information). The mechanical properties of DHNP@BSA-X and PNP@BSA-X were assessed by rheometry (Figure S7C in Supporting Information), confirming that both cross-linked hydrogels exhibited a higher storage modulus (G′) than the loss modulus (G″), indicative of solid-like properties. Release from DHNP@BSA-X and PNP@BSA-X was significantly slower than that of the respective free drugs ($p < 0.0001$ at 24 h).

2.3. Sciatic nerve blockade

We injected 0.3 ml of various formulations at the left sciatic nerve and conducted neurobehavioral testing to evaluate the duration of sensory and motor functional deficits, in both hind paws (Fig. 3, Figure S8 and Figure S9 in Supporting Information). Deficits in the left (injected) hindpaw reflect nerve block, while deficits in the right (uninjected) hindpaw reflect effects of systemically distributed bupivacaine [38,39]. Importantly, none of the formulations caused deficits in the uninjected hindpaw throughout the study (Figure S9 in Supporting Information).

BSA (50 mg/ml) and BSA-X did not cause any nerve block in the absence of bupivacaine (Fig. 3). Bupivacaine at 5 mg/ml – 0.5 % v/w, a concentration in common clinical use – achieved a sensory block duration of 2.6 h. Block from 5 mg/ml BNP in uncrosslinked BSA (BNP@BSA) lasted 2.5 h ($p = 0.827$ compared to free bupivacaine). The duration of sensory block from BNP@BSA did not have a statistically significant increase with increasing bupivacaine nanoparticle concentration (2.9 h for 10 mg/ml and 3.8 h for 20 mg/ml). Cross-linking the BSA (BNP@BSA-X) markedly increased the duration of block at every bupivacaine loading. The durations of block were 4.2-fold longer at 5 mg/ml bupivacaine ($p = 0.077$), 6.4-fold at 10 mg/ml ($p = 0.011$), and 10.6-fold at 20 mg/ml ($p < 0.0001$). At 20 mg/ml bupivacaine, BNP@BSA-X achieved 39.9 h nerve block. By way of comparison, the duration achieved by the same volume of commercially available 13.3 mg/ml bupivacaine liposomes (EXPAREL®) was 5.1 h, i.e., 8-fold shorter ($p < 0.0001$).

Sensory nerve block with 20 mg/ml bupivacaine•HCl@BSA-X (7.3 h) was 5.4-fold shorter than with BNP@BSA-X (39.9 h, $p < 0.0001$), demonstrating the importance of the nanoformulation of bupivacaine. This observation is consistent with the *in vitro* release kinetics (Fig. 1F).

There was no difference in the durations of sensory and motor block for any formulation (Figure S8 in Supporting Information).

2.4. Tissue retention

To evaluate drug retention in tissue, we employed the hydrophobic near-infrared (NIR) dye indocyanine green (ICG) as a model drug (excitation 790 nm, emission 810 nm). Nanoparticles containing ICG and bupivacaine nanoparticle (ICG-BNP) were formed by the same process as for BNP except that ICG was co-dissolved in methanol with bupivacaine free base. When free ICG and ICG-BNP@BSA were injected at the sciatic nerve (Fig. 4A and B), the associated fluorescence became undetectable within 24 h. Cross-linking of the BSA markedly enhanced retention of ICG. With cross-linked BSA, release of ICG incorporated in BNP (ICG-BNP@BSA-X) was slower than from ICG incorporated in bupivacaine•HCl (ICG-bupivacaine•HCl@BSA-X) (51 % vs. 82 % respectively at 28 days, $p = 0.006$). These data suggest that both nanoformulation and the cross-linking of BSA contributed to prolonging retention in tissue.

To track tissue retention of BSA-X, the dye Cy5.5 was bound covalently to BSA (Cy5.5-BSA; excitation 660 nm, emission 710 nm). When free Cy5.5 or non-cross-linked cy5.5-BSA containing BNP (BNP@ Cy5.5-BSA) was injected at the sciatic nerve, the associated fluorescence decreased by approximately 80 % within 7 days. In contrast, when BSA was crosslinked (BNP@Cy5.5-BSA-X), the fluorescence decreased by only 36.2 % over the same period ($p = 0.004$ when comparing to free Cy5.5 and $p = 0.005$ when comparing to BNP@Cy5.5-BSA; Fig. 4C and D).

The duration of the nerve block from formulations correlated ($R^2 = 0.9949$) with the half-life of tissue retention (calculated from data in Fig. 4B) of the model drug ICG (Fig. 5A). (The half-life is the time to a 50 % reduction in fluorescence relative intensity.) The durations of nerve block and tissue retention from bupivacaine•HCl@BSA-X were much shorter than from BNP@BSA-X, supporting the importance of nanoformulation. Notably, the duration of nerve block and tissue retention from crosslinked BSA (BNP@BSA-X and bupivacaine•HCl@BSA-X) were much longer than from non-crosslinked BSA (BNP@BSA), confirming the importance of BSA cross-linking. The duration of nerve block also correlated ($R^2 = 0.9593$) with the percentage of fluorescence relative intensity of Cy5.5 dye remaining on day 2 (Fig. 5B), as calculated from data in Fig. 4D. In particular, cross-linking of BSA (BNP@BSA-X vs. BNP@BSA) was associated with much longer duration of block.

ICG was retained in tissue longer with ICG-BNP@BSA-X than with ICG-BNP@BSA, BSA was retained longer with in BNP@Cy5.5-BSA-X than BNP@Cy5.5-BSA, and nerve block was longer with formulations with BSA-X. These findings are consistent with the view that cross-linking of BSA slows release from BNPs, and that the similarity of the release of bupivacaine from BNP@BSA and BNP@BSA-X *in vitro* (Fig. 1F) is due to restriction of the diffusion of BSA by the dialysis membrane.

2.5. Tissue reaction

Tissue reaction was assessed 4 days after the injection of BNP@BSA-X (20 mg/ml bupivacaine), a time frame when acute inflammation and muscle injury are typically well-established following perineural injection of drugs and biomaterials (Fig. 6) [9]. The

sciatic nerves and adjacent tissues were harvested, processed into hematoxylin-eosin (H&E) stained sections and inflammation and myotoxicity were assessed (inflammation scores 0–4; myotoxicity scores 0–6). In all rats treated with BNP@BSA-X, discrete eosinophilic deposits (indicating protein) were found in close proximity to the sciatic nerve (Fig. 6A). On histological examination, the response to BNP@BSA-X was characterized by a mixed inflammatory infiltrate (median score: 2) primarily composed of macrophages, along with a smaller population of lymphocytes and occasional neutrophils in the soft tissues surrounding the muscle. BNP@BSA-X caused mild myotoxicity (median score: 1), with degenerating and regenerating myocytes predominantly located in perifascicular muscle. Injection of the same volume of the commercially available EXPAREL® (bupivacaine concentration 13.3 mg/ml[40]), had a similar degree of inflammation (median score: 2, $p = 0.5$) but had more myotoxicity (median score: 3, $p = 0.019$).

3. Discussion

We have engineered an injectable depot platform of drug nanoparticles within a protein-based hydrogel system that is formed by a one-pot synthesis that does not require additional purification steps. We demonstrate that it could be applied to three different small molecule drugs. We provide proof of concept *in vivo* with the local anesthetic bupivacaine, and demonstrate that this system can provide very prolonged nerve block.

For *in vivo* demonstration of safety and efficacy, we used sciatic nerve blockade with bupivacaine, a commonly used relatively long-acting local anesthetic. The nanoparticulate and cross-linked protein components were both important in achieving prolonged nerve block. The effect of nanoformulation of BNP on release kinetics was at least in part due to the fact that the bupivacaine was in hydrophobic free base form, which would slow diffusion away from the depot. BSA slowed release by binding of bupivacaine nanoparticles [23]. Drug binding to BSA may have had a greater effect than cross-linking per se, as evidenced by the fact that bupivacaine release was similar for BNP@BSA and BNP@BSA-X *in vitro*, i.e., when diffusion/dilution of BSA was prevented by containment within a dialysis membrane. However, BNP@BSA-X resulted in much longer block durations than BNP@BSA *in vivo*, where disappearance of BSA from the site of injection was not limited. Moreover, the micron-scale pore size of BSA-X is unlikely to have a marked effect on diffusion of bupivacaine. This view is supported by the experience with cross-linked hyaluronic acid hydrogels, which had a relatively modest effect on the release and duration of block from bupivacaine hydrochloride, and had a similar pore size to BSA-X [41, 42]. Incorporation of BNP within BSA-X could also have an effect by slowing removal of nanoparticles from the site of injection [43].

Injectable drug delivery systems almost invariably entail local inflammation [44,45]. When they deliver conventional local anesthetics, there is also myotoxicity [2,9,10,40,46,47]. Although such injury generally recovers spontaneously, it is not desirable and can result in serious injury [46,48]. At high concentrations of local anesthetics or particularly toxic compounds, there can be nerve injury [46,49–51]. The concentration of local anesthetic administered is a primary determinant of tissue injury. We have argued that tissue reaction can be a limiting factor with sustained release systems for conventional local anesthetics,

preventing the achievement of very long block [46]. Here, nerve block from BNP@BSA-X lasted 8 times longer than block from EXPAREL® (13.3 mg/ml bupivacaine), a commercially available liposomal bupivacaine product, and had comparable or better tissue reaction [40], even though it contained more bupivacaine (20 mg/ml). Also of note, none of the animals tested had neurobehavioral deficits in the contralateral (un-injected) hindpaw, suggesting that there was no effect from systemically distributed drug. This is important because of the potential for systemic toxicity with conventional local anesthetics [38].

The systemic toxicity of a given dose of a drug decreases (often linearly) with increasing mass and volume of the animal to which it is administered, while the local anesthetic efficacy diminishes much less with increasing mass [38]. Moreover, as animals increase in size, it is possible to inject more mass of a drug delivery system. Consequently, the duration of block from sustained release local anesthetic systems might be longer in humans than it was here in rats (~200-fold difference in mass). The potential for longer blocks in humans is seen in the fact that a polymeric microspheres delivering bupivacaine and dexamethasone caused nerve block lasting ~2 days, while the same formulation in sheep lasted ~13 days [52]. These considerations and our data suggest the potential for prolonged and safe local anesthesia.

In sustained release systems for conventional local anesthetics, the biomaterial and the drugs can cause inflammation which lasts as long as there is residual material present [9]. The inflammation resolves completely when both are gone, with no apparent sequelae [51]. The local anesthetic itself can also cause myotoxicity, which also resolves completely once the drug is gone [9]. This resolution was verified through histological examination conducted 30 days post-injection of BNP@BSA-X (Figure S10 in Supporting Information).

4. Materials and methods

4.1. Reagents

All materials and reagents, unless otherwise noted, were purchased from Sigma-Aldrich (St. Louis, MO, USA), and used as received.

4.2. Synthesis of bupivacaine free base

Bupivacaine hydrochloride was dissolved in 50 ml of deionized water, and a 0.2 M NaOH solution was slowly added under stirring. The free base form began to precipitate as a white solid, and the NaOH solution was continuously added until a pH of 11 was achieved (pKa = 8.4). The resulting white solid was filtered under vacuum and washed with deionized water multiple times. The solid was subsequently dried under vacuum overnight.

4.3. Preparation of bupivacaine nanoparticle (BNP) in PBS

Adding bupivacaine free base directly to PBS without BSA resulted in immediate aggregation, especially at a high concentration of bupivacaine free base (20 mg/ml) (Figure S11 in Supporting Information). In Fig. 1F–a low concentration (5 mg/ml) of bupivacaine free base was used for the BNP, as this concentration did not result in immediate aggregation.

4.4. Preparation of bupivacaine nanoparticle (BNP) in BSA-X (BNP@BSA-X)

Bupivacaine free base was dissolved in methanol to prepare a stock solution. Bovine serum albumin (BSA) was dissolved in pH 7.4 phosphate-buffered saline (PBS). The BSA solution was vigorously stirred while rapidly adding the bupivacaine free base solution. Methanol was removed by rotary evaporation. Subsequently, glutaraldehyde (GA) was added to the solution at a final concentration of 5 mg/ml or 10 mg/ml to create the a BSA hydrogel with embedded bupivacaine nanoparticles (BNP@BSA-X).

4.5. Detection of residual glutaraldehyde (GA) in BNP@BSA-X samples

As glutaraldehyde lacks a chromophore, we chemically modified both aldehyde functional groups of GA with 2,4-dinitrophenylhydrazine (DNPH), forming DNPH-GA, which could be detected by HPLC by measuring absorbance at 365 nm [33].

To prepare the 2,4-dinitrophenylhydrazine (DNPH) standard solution, 5 mg of DNPH was added to 25 μl of 85 % phosphoric acid, followed by the addition of 5 ml acetonitrile (ACN) to create a 1 mg/ml DNPH standard solution. The solution was shaken until fully dissolved.

10 mg of BNP@BSA-X was placed in 1 ml of PBS. After 24 h, 50 μl of the supernatant was collected then added to 2 ml of DNPH standard solution (1 mg/ml), and acetonitrile (ACN) was added to reach a final volume of 5 ml. This sample was then analyzed by HPLC.

To establish the standard curve, 50 μl of a 500 mg/ml GA solution was diluted with 5 ml ACN to prepare a 1 mg/ml GA stock solution. Subsequently, 50 μl of the GA stock solution (1 mg/ml) was added to 2 ml of DNPH standard solution, and ACN was added to reach a final volume of 5 ml, making DNPH modified GA (DNPH-GA) stock solution (10 μg/ml of GA concentration).

Each dilution of DNPH-GA stock solution (0.01, 0.1, 0.5, and 1 μg/ml of GA concentration) was injected into the HPLC system (Agilent 1260 Infinity, Agilent, Santa Clara, CA, USA) equipped with a C18 column (Poroshell 120 EC-C18, 4.6 × 100 mm, i.d. 2.7 μm, Agilent, Santa Clara, CA, USA) using an acetonitrile/water (75:25) mobile phase at a flow rate of 0.5 ml min^{-1}. Detection of DNPH-GA was achieved through UV absorbance at λ = 365 nm. The calibration curve was generated using concentrations of 0.01, 0.1, 0.5, and 1 μg/ml of GA (Figure S3 in Supporting Information).

In the supernatant of BNP@BSA-X, no peak for DNPH-GA was observed, confirming the absence of residual glutaraldehyde in the BNP@BSA-X after synthesis.

4.6. Preparation of diphenhydramine nanoparticle (DHNP) in BSA-X (DHNP@BSA-X)

Diphenhydramine hydrochloride was dissolved in methanol at a concentration of 100 mg/ml, and triethylamine (TEA) was added at a volume ratio of 1 % (v/v). After 30 min of stirring, this solution was introduced into the BSA solution, previously prepared in pH 7.4 PBS at a concentration of 50 mg/ml. This addition resulted in a final diphenhydramine concentration of 1 mg/ml. Methanol was removed by rotary evaporation. Subsequently, GA was added to the solution at a final concentration of 5 mg/ml to create the diphenhydramine nanoparticle-embedded hydrogel, denoted as DHNP@BSA-X.

4.7. Preparation of paclitaxel nanoparticle (PNP) in BSA-X(PNP@BSA-X)

Paclitaxel was dissolved in methanol to create a stock solution with a concentration of 100 mg/ml. Concurrently, bovine serum albumin (BSA) was dissolved in pH 7.4 phosphate-buffered saline (PBS) at a concentration of 50 mg/ml. The BSA solution was vigorously stirred while the paclitaxel solution was added to reach a final paclitaxel concentration of 1 mg/ml. Methanol was removed by rotary evaporation. Subsequently, GA was added to the solution at a final concentration of 5 mg/ml to create the paclitaxel nanoparticle-embedded hydrogel, denoted as PNP@BSA-X.

4.8. General method to prepare BSA gel (BSA-X)

500 mg/ml glutaraldehyde (GA) in water was added to the stirring BSA protein solution to achieve the desired final concentration of 5 mg/ml or 10 mg/ml.

4.9. Preparation of bupivacaine•HCl in BSA (Bupivacaine•HCl@BSA)

To prepare bupivacaine•HCl in BSA (Bupivacaine•HCl@BSA), the bupivacaine•HCl was dissolved in water, and then a solution of BSA in a pH 7.4 buffer was added to the mixture. The resulting mixture was then stirred to create Bupivacaine•HCl@BSA.

4.10. Preparation of ICG and BNP in BSA (ICG-BNP@BSA)

A stock solution was prepared by dissolving ICG (0.5 mg/ml) and Bupivacaine free base (200 mg/ml) in methanol. In a separate solution, bovine serum albumin (BSA) (50 mg/ml) was dissolved in pH 7.4 phosphate-buffered saline (PBS) and vigorously stirred. The Bupivacaine free base and ICG solution were then added to the BSA solution while stirring. The final concentration of BNP and ICG was 20 mg/ml and 0.05 mg/ml, respectively. Methanol was removed by rotary evaporation.

4.11. Preparation of ICG and bupivacaine•HCl in BSA hydrogel (ICG-Bupivacaine•HCl @BSA-X)

To prepare ICG and bupivacaine•HCl in BSA, a solution was created by dissolving both ICG and bupivacaine•HCl in BSA solution. The resulting solution was then treated with addition of a 500 mg/ml glutaldehyde solution in water to achieve the desired final concentration of 5 mg/ml.

4.12. Preparation of BNP in Cy5.5 dye conjugated BSA hydrogel (BNP@Cy5.5-BSA-X)

Bupivacaine free base was dissolved in methanol to prepare a stock solution. Then, a solution of Cy5.5 dye-conjugated BSA (Cy5.5-BSA, purchased from Nanocs Inc, New York, NY, USA) was mixed with BSA to create a mixture with a final concentration of 50 mg/ml BSA. The concentration of Cy5.5 dye in the solution was 0.05 mg/ml. The mixture was vigorously stirred while the bupivacaine free base was added. Methanol was removed by rotary evaporation. The resulting solution was then treated with addition of a 500 mg/ml glutaldehyde solution in water to achieve the desired final concentration of 5 mg/ml.

4.13. Dynamic light scattering (DLS)

The particle size was measured with a Malvern Nano ZetaSizer (Malvern Panalytical, Westborough, MA, USA).

4.14. Transmission electron microscopy (TEM)

The BNP@BSA solution was prepared by subjecting it to centrifugation to remove any excess BSA protein. The resulting pellet was then washed three times and resuspended in water. Carbon-coated 400 mesh copper grids (Ted Pella, Inc., Redding, CA, USA) were subjected to glow charging for 90 s before BNP@BSA solution were deposited on them. A volume of 5 μl of resuspended BNP@BSA was placed on the grid and allowed to settle for 5 min. The grid was then washed with distilled water, stained with 1 % (w/w) uranyl acetate, and wicked dry with filter paper. Transmission electron microscopy (TEM) images were acquired using a Tecnai G2 Spirit BioTWIN transmission electron microscope (FEI company, Hillsboro, OR, USA) operating at an acceleration voltage of 80 kV.

4.15. Scanning electron microscope (SEM)

The surface morphology of the hydrogel was examined using a Hitachi S-4700 Field Emission Scanning Electron Microscope (FE-SEM) at an accelerating voltage of 10 kV and 12 μA. The BSA hydrogel was prepared, flash-frozen in liquid nitrogen, and subsequently lyophilized. Prior to imaging, the sample cross-sections were obtained using a razor blade and mounted on SEM stubs with double-sided carbon tape. To enhance conductivity, the samples were further coated with an Au/Pd alloy using sputter coating techniques.

4.16. Rheological testing

The rheological characteristics of the formulations were evaluated by means of a TA DHR-2 rheometer (TA instruments, NewCastle, DE, USA) furnished with a temperature regulator. A parallel plate with a diameter of 20 mm was implemented in all tests. The distance between the plates was set at 0.3 mm. Frequency sweeps were conducted within the range of 0.63–628 rad/s with a strain of 0.1 %. The choice of 10^2 rad/s in Fig. 1D is based on its alignment within the range associated with muscle tremor and vibration (62.83–251.3 rad/s), synchronized with the central nervous system [53]. Step-strain oscillation tests were performed with a shear strain of 0.1 % for 60 s, followed by 500 % for 60 s, repeated for three cycles at a frequency of 6.28 rad/s. All measurements were taken at 25 °C.

4.17. In vitro drug release for bupivacaine and diphenhydramine containing formulations

Drug release was performed by placing test formulations (Bupivacaine•HCl (5 mg/ml), Bupivacaine•HCl@BSA (5 mg/ml), Bupivacaine•HCl@BSA-X (20 mg/ml), BNP (5 mg/ml), BNP@BSA (20 mg/ml), BNP@BSA-X (20 mg/ml); the value inside the parentheses represents the concentration of bupivacaine. Diphenhydramine•HCl (1 mg/ml), DHNP@BSA-X (1 mg/ml); the value inside the parentheses represents the concentration of diphenhydramine.) into a Slide-A-Lyzer MINI dialysis device (Thermo Fisher Scientific, Waltham, MA, USA) with a 3000 MW cut-off, further dialyzed with 14 ml 0.9 % saline and incubated at 37 °C on a Isotemp Incubator (Fisher Scientific, Hampton, NH, USA). The concentration of at each time point, the dialysis solution was exchanged with fresh,

pre-warmed 0.9 % saline. 0.5 ml of the dialysis solution was saved for drug analysis. The concentration of bupivacaine or diphenhydramine in release media was quantified by HPLC (Agilent 1260 Infinity, Agilent, Santa Clara, CA, USA) using a C18 column (Poroshell 120 EC-C18, 4.6 × 100 mm, i.d. 2.7 μm, Agilent, Santa Clara, CA, USA) with a acetonitrile/water (60:40) mobile phase and a flow rate of 0.5 ml min^{-1} [54–57]. Bupivacaine and diphenhydramine was detected by UV absorbance at $\lambda = 250$ nm. The drug release half-time was calculated based on the time taken for the released drug accumulation equals to half of the drug loaded.

4.18. In vitro release kinetics for paclitaxel containing formulations

Drug release were performed by placing test formulations (Paclitaxel (1 mg/ml), PNP@BSA-X (1 mg/ml), the value inside the parentheses represents the concentration of paclitaxel) into a Slide-A-Lyzer MINI dialysis device (Thermo Fisher Scientific, Waltham, MA, USA) with a 3000 MW cut-off, further dialyzed with 14 ml 0.9 % saline and incubated at 37 °C on a Isotemp Incubator (Fisher Scientific, Hampton, NH, USA). The concentration of at each time point, the dialysis solution was exchanged with fresh, pre-warmed 0.9 % saline. 0.5 ml of the dialysis solution was saved for drug analysis. The concentration of paclitaxel in release media was quantified by UV–Vis spectrometer (Agilent Cary UV–Vis Compact Peltier, Agilent, Santa Clara, CA, USA) at 224 nm.

4.19. Analysis of interaction between BNP and BSA by fluorimetry

All fluorescence measurements were conducted using a BioTek® Synergy™ Mx microplate reader (BioTek, Winooski, VT, USA). Fluorescence spectra at 37 °C were recorded from 310 to 450 nm with an excitation wavelength of 280 nm. The excitation and emission slit widths were set to 9 nm. In these measurements, the concentration of BSA was maintained at 1 mg/ml in PBS, while the concentrations of BNP were 0.05, 0.1, and 0.2 mg/ml. As a control, fluorescence was measured for 0.2 mg/ml of BNP in PBS.

4.20. Interaction between BNP and BSA using UV–vis spectrometry

UV–vis absorption spectra at 37 °C were recorded on a UV–Vis spectrometer (Agilent Cary UV–Vis Compact Peltier, Agilent, Santa Clara, CA, USA) across a wavelength range of 190–350 nm. The concentration of BSA was fixed at 1 mg/ml in PBS, and the concentrations of BNP were 0.02, 0.04, 0.06, and 0.08 mg/ml. As a control, UV–Vis absorption was measured for 0.08 mg/ml of BNP in PBS.

4.21. Animal care and studies

All experiments were conducted in accordance with the Boston Children’s Hospital Animal Care and Use Committee in accordance with the guidelines of the International Association for the Study of Pain. Adult male Sprague-Dawley rats were purchased from the Charles River Laboratories (Wilmington, MA, USA) weighing 300–400g were housed in groups under a 12-hr/12-hr light/dark cycle with lights on at 6:00 AM.

4.22. In vivo imaging system (IVIS) imaging

Rats were administered 0.3 ml of each formulation under isoflurane-oxygen anesthesia and subsequently shaved. *In vivo* fluorescence images were captured at predetermined time points post-injection, with fluorescence intensity evaluated using a Spectrum IVIS (PerkinElmer, Waltham, MA, USA) under brief isoflurane-oxygen anesthesia. Whole body animal images were recorded non-invasively using the following settings: excitation 780 nm, emission 845 nm (Free ICG, ICG-BNP@BSA, ICG-B@BSA-X, ICG-BNP@BSA-X); excitation 660 nm, emission 710 nm (Free Cy5.5, BNP@Cy5.5-BSA, BNP@Cy5.5-BSA-X).

4.23. Sciatic nerve block

Injections at the left sciatic nerve were administered using a 23-gauge needle under brief anesthesia with isoflurane-oxygen. The needle was inserted in a postero-medial direction to the greater trochanter, pointing in an anteromedial direction. Upon contact with bone, the formulations were injected. Neurobehavioral testing was conducted on both hindquarters. Deficits in the left extremity reflected nerve block, deficits in the right (uninjected) extremity were used as an indicator of systemic drug distribution. Sensory nerve blockade was assessed using a modified hotplate test. In brief, the hind paws were exposed sequentially (left then right) to a 56 °C hotplate (Stoelting, Wood Dale, IL, USA), and the time the animal allowed its paw to remain on the hotplate (thermal latency) was measured. A thermal latency of 2 s indicated no nerve blockade (baseline), and a thermal latency of 12 s was considered maximal latency. Successful nerve blockade was defined as achieving a thermal latency above 7 s. The hind paws were removed from the hotplate after 12 s to prevent thermal injury. Measurements were repeated three times in each animal at each time point, and the median was used for data analysis.

Motor nerve block was assessed using a weight-bearing test to determine the motor strength of the rat's hind-paw. In brief, the rat was positioned with one hind-paw on a digital balance and allowed to bear its weight. The maximum weight that the rat could bear without the ankle touching the balance was recorded, and motor block was considered achieved when the motor strength was less than half-maximal. Measurements were repeated three times at each time point, and the median was used for further data analysis.

The duration of sensory block was calculated as the time required for thermal latency to return to 7 s (halfway between baseline and maximal latencies). The duration of motor block was defined as the time it took for weight-bearing to return to halfway between normal and maximal block.

4.24. Tissue harvesting and histology

At 4 days and 28days after injection, rats were sacrificed to evaluate both acute and chronic inflammation and myotoxicity. The sciatic nerve was harvested along with surrounding tissues, and the dissector was blinded to the solution injected into each rat. Muscle samples were fixed in 10 % neutral buffered formalin, and standard techniques were employed to process them for histology (hematoxylin-eosin stained slides). An observer blinded to individual sample nature analyzed the slides. The specimens were scored for inflammation

(0–4 points) and myotoxicity (0–6 points), where inflammation severity was subjectively assessed as: 0, no inflammation; 1, peripheral inflammation; 2, deep inflammation; 3, muscular hemifascicular inflammation; 4, muscular holofascicular inflammation. Myotoxicity was scored based on two characteristic features of local anesthetic myotoxicity, namely nuclear internalization and regeneration. Nuclear internalization refers to myocytes with nuclei located away from their usual position at the cell periphery but with normal size and chromicity. Regeneration refers to shrunken myocytes with scant eosinophilic cytoplasm and hyper-chromatic nuclei. Scoring ranged from 0 (normal) to 6 (holofascicular regeneration), with the grade for a sample indicating the worst area (most severe damage) present on the slide.

4.25. Statistical analysis

The statistical analysis was performed using Prism 7 statistical software (GraphPad Software, San Diego, CA, USA), and a two-sided Student's t-test was used unless otherwise specified. Differences between groups were considered statistically significant when $p \leq 0.05$. Statistical significance was defined as follows: *ns* ($p > 0.05$), * ($p \leq 0.05$), ** ($p \leq 0.01$), *** ($p \leq 0.001$), and **** ($p \leq 0.0001$).

Supplementary Material

Refer to Web version on PubMed Central for supplementary material.

Acknowledgments

This research was funded by NIH R35 GM131728 (to D.S.K.).

Data availability

Data will be made available on request.

References

[1]. Becker DE, Reed KL, Local anesthetics: review of pharmacological considerations, Anesth. Prog 59 (2) (2012) 90–101, quiz 102–3. [PubMed: 22822998]

[2]. Santamaria CM, Woodruff A, Yang R, Kohane DS, Drug delivery systems for prolonged duration local anesthesia, Mater. Today 20 (1) (2017) 22–31.

[3]. Hoare T, Young S, Lawlor MW, Kohane DS, Thermoresponsive nanogels for prolonged duration local anesthesia, Acta Biomater. 8 (10) (2012) 3596–3605. [PubMed: 22732383]

[4]. Epstein-Barash H, Shichor I, Kwon AH, Hall S, Lawlor MW, Langer R, Kohane DS, Prolonged duration local anesthesia with minimal toxicity, Proc. Natl. Acad. Sci. U. S. A 106 (17) (2009) 7125–7130. [PubMed: 19365067]

[5]. Sulaiman L, Macfarlane RJ, Waseem M, Current concepts in anaesthesia for shoulder surgery, Open Orthop. J 7 (2013) 323–328. [PubMed: 24082970]

[6]. Beecroft CL, Coventry DM, Anaesthesia for shoulder surgery, Cont. Educ. Anaesth. Crit. Care Pain 8 (6) (2008) 193–198.

[7]. Kohane DS, Smith SE, Louis DN, Colombo G, Ghoroghchian P, Hunfeld NG, Berde CB, Langer R, Prolonged duration local anesthesia from tetrodotoxin-enhanced local anesthetic microspheres, Pain 104 (1–2) (2003) 415–421. [PubMed: 12855352]

[8]. Cullion K, Petishnok LC, Ji T, Zurakowski D, Kohane DS, The duration of nerve block from local anesthetic formulations in male and Female rats, Pharm. Res. (N. Y.) 36 (12) (2019) 179.

[9]. Kohane DS, Lipp M, Kinney RC, Anthony DC, Louis DN, Lotan N, Langer R, Biocompatibility of lipid-protein-sugar particles containing bupivacaine in the epineurium, J. Biomed. Mater. Res 59 (3) (2002) 450–459. [PubMed: 11774302]

[10]. Padera R, Bellas E, Tse JY, Hao D, Kohane DS, Local myotoxicity from sustained release of bupivacaine from microparticles, Anesthesiology 108 (5) (2008) 921–928. [PubMed: 18431129]

[11]. Davidson AM, Brust M, Cooper DL, Volk M, Sensitive analysis of protein Adsorption to Colloidal gold by Differential centrifugal Sedimentation, Anal. Chem 89 (12) (2017) 6807–6814. [PubMed: 28513153]

[12]. Baki A, Remmo A, Lowa N, Wiekhorst F, Bleul R, Albumin-coated Single-core Iron Oxide nanoparticles for enhanced molecular Magnetic imaging (MRI/MPI), Int. J. Mol. Sci 22 (12) (2021).

[13]. Brewer SH, Glomm WR, Johnson MC, Knag MK, Franzen S, Probing BSA binding to citrate-coated gold nanoparticles and surfaces, Langmuir 21 (20) (2005) 9303–9307. [PubMed: 16171365]

[14]. Dominguez-Medina S, Blankenburg J, Olson J, Landes CF, Link S, Adsorption of a protein Monolayer via hydrophobic interactions prevents nanoparticle aggregation under Harsh Environmental Conditions, ACS Sustain. Chem. Eng 1 (7) (2013) 833–842. [PubMed: 23914342]

[15]. Ma X, Sun X, Hargrove D, Chen J, Song D, Dong Q, Lu X, Fan TH, Fu Y, Lei Y, A Biocompatible and Biodegradable protein hydrogel with green and red Autofluorescence: Preparation, characterization and in vivo Biodegradation tracking and modeling, Sci. Rep 6 (2016) 19370. [PubMed: 26813916]

[16]. Raghuwanshi VS, Yu B, Browne C, Garnier G, Reversible pH responsive bovine serum albumin hydrogel Sponge Nanolayer, Front. Bioeng. Biotechnol 8 (2020) 573. [PubMed: 32582681]

[17]. Yasun E, Li C, Barut I, Janvier D, Qiu L, Cui C, Tan W, BSA modification to reduce CTAB induced nonspecificity and cytotoxicity of aptamer-conjugated gold nanorods, Nanoscale 7 (22) (2015) 10240–10248. [PubMed: 25990591]

[18]. Weigert F, Muller A, Hausler I, Geissler D, Skroblin D, Krumrey M, Unger W, Radnik J, Resch-Genger U, Combining HR-TEM and XPS to elucidate the coreshell structure of ultrabright CdSe/CdS semiconductor quantum dots, Sci. Rep 10 (1) (2020) 20712. [PubMed: 33244030]

[19]. Denson D, Coyle D, Thompson G, Myers J, Alpha 1-acid glycoprotein and albumin in human serum bupivacaine binding, Clin. Pharmacol. Ther 35 (3) (1984) 409–415. [PubMed: 6697648]

[20]. Terasaki T, Pardridge WM, Denson DD, Differential effect of plasma protein binding of bupivacaine on its in vivo transfer into the brain and salivary gland of rats, J. Pharmacol. Exp. Therapeut 239 (3) (1986) 724–729.

[21]. Ghoneim MM, Pandya H, Plasma protein binding of bupivacaine and its interaction with other drugs in man, Br. J. Anaesth 46 (6) (1974) 435–438. [PubMed: 4458761]

[22]. Mather LE, Thomas J, Bupivacaine binding to plasma protein fractions, J. Pharm. Pharmacol 30 (10) (1978) 653–654. [PubMed: 30824]

[23]. Galenko-Yaroshevskii AP, Fistunenko PN, Dukhanin AS, Kinetics of interaction of local anesthetics with human serum albumin, Bull. Exp. Biol. Med 140 (3) (2005) 315–316. [PubMed: 16307046]

[24]. Wani TA, Bakheit AH, Abounassif MA, Zargar S, Study of interactions of an Anticancer drug Neratinib with bovine serum albumin: spectroscopic and molecular docking approach, Front. Chem 6 (2018) 47. [PubMed: 29564326]

[25]. Pawar SK, Jaldappagari S, Interaction of repaglinide with bovine serum albumin: spectroscopic and molecular docking approaches, J Pharm Anal 9 (4) (2019) 274–283. [PubMed: 31452966]

[26]. El Gammal RN, Elmansi H, El-Emam AA, Belal F, Elzahhar PA, Belal ASF, Hammouda MEA, Insights on the in-vitro binding interaction between donepezil and bovine serum albumin, BMC Chem 17 (1) (2023) 31. [PubMed: 37024940]

[27]. El Gammal RN, Elmansi H, El-Emam AA, Belal F, Hammouda MEA, Exploring the molecular interaction of mebendazole with bovine serum albumin using multi-spectroscopic approaches and molecular docking, Sci. Rep 12 (1) (2022) 11582. [PubMed: 35804178]

[28]. Liu J, He Y, Liu D, He Y, Tang Z, Lou H, Huo Y, Cao X, Characterizing the binding interaction of astilbin with bovine serum albumin: a spectroscopic study in combination with molecular docking technology, RSC Adv. 8 (13) (2018) 7280–7286. [PubMed: 35540350]

[29]. Aroche DMP, Vargas JP, Nogara PA, da Silveira Santos F, da Rocha JBT, Ludtke DS, Rodembusch FS, Glycoconjugates based on Supramolecular Troger's base Scaffold: synthesis, Photophysics, docking, and BSA association study, ACS Omega 4 (8) (2019) 13509–13519. [PubMed: 31460480]

[30]. Raeisi Vanani A, Asadpour S, Aramesh-Boroujeni Z, Mobini Dehkordi M, Studying the interaction between the new neodymium (Nd) complex with the ligand of 1,10-phenanthroline with FS-DNA and BSA, Front. Chem 11 (2023) 1208503.

[31]. Xu H, Yao N, Xu H, Wang T, Li G, Li Z, Characterization of the interaction between eupatorin and bovine serum albumin by spectroscopic and molecular modeling methods, Int. J. Mol. Sci 14 (7) (2013) 14185–14203. [PubMed: 23839090]

[32]. Alanazi AM, Abdelhameed AS, A spectroscopic approach to investigate the molecular interactions between the Newly Approved irreversible ErbB blocker "Afatinib" and bovine serum albumin, PLoS One 11 (1) (2016) e0146297. [PubMed: 26751077]

[33]. Maggadani BP, Harmita, Isfadhila M, High-performance liquid chromatography Analytical method Validation for glutaraldehyde and Benzalkonium Chloride in Disinfectants, Int. J. Appl. Pharm 10 (1) (2018).

[34]. Hoare T, Santamaria J, Goya GF, Irusta S, Lin D, Lau S, Padera R, Langer R, Kohane DS, A magnetically triggered composite membrane for on-demand drug delivery, Nano Lett. 9 (10) (2009) 3651–3657. [PubMed: 19736912]

[35]. Nandgude TD, Bhise KS, Gupta VB, Characterization of hydrochloride and tannate salts of diphenhydramine, Indian J. Pharmaceut. Sci 70 (4) (2008) 482–486.

[36]. Bartzatt R, Comparative analysis of antihistamines and Nonsteroidal anti-inflammatory drugs (NSAIDs): properties, structure and Prediction of new potential drugs, J Adv Med Pharm 12 (3) (2017) 1–18.

[37]. Sharma S, Verma A, Teja BV, Shukla P, Mishra PR, Development of stabilized Paclitaxel nanocrystals: in-vitro and in-vivo efficacy studies, Eur. J. Pharmaceut. Sci 69 (2015) 51–60.

[38]. Kohane DS, Sankar WN, Shubina M, Hu D, Rifai N, Berde CB, Sciatic nerve blockade in infant, adolescent, and adult rats: a comparison of ropivacaine with bupivacaine, Anesthesiology 89 (5) (1998) 1199–1208. ; discussion 10A. [PubMed: 9822009]

[39]. Thalhammer JG, Vladimirova M, Bershadsky B, Strichartz GR, Neurologic evaluation of the rat during sciatic nerve block with lidocaine, Anesthesiology 82 (4) (1995) 1013–1025. [PubMed: 7717536]

[40]. McAlvin JB, Padera RF, Shankarappa SA, Reznor G, Kwon AH, Chiang HH, Yang J, Kohane DS, Multivesicular liposomal bupivacaine at the sciatic nerve, Biomaterials 35 (15) (2014) 4557–4564. [PubMed: 24612918]

[41]. Yeo Y, Highley CB, Bellas E, Ito T, Marini R, Langer R, Kohane DS, In situ cross-linkable hyaluronic acid hydrogels prevent post-operative abdominal adhesions in a rabbit model, Biomaterials 27 (27) (2006) 4698–4705. [PubMed: 16750564]

[42]. Jia X, Colombo G, Padera R, Langer R, Kohane DS, Prolongation of sciatic nerve blockade by in situ cross-linked hyaluronic acid, Biomaterials 25 (19) (2004) 4797–4804. [PubMed: 15120526]

[43]. Yeo Y, Ito T, Bellas E, Highley CB, Marini R, Kohane DS, In situ cross-linkable hyaluronan hydrogels containing polymeric nanoparticles for preventing postsurgical adhesions, Ann. Surg 245 (5) (2007) 819–824. [PubMed: 17457177]

[44]. Bernatchez SF, Merkli A, Minh TL, Tabatabay C, Anderson JM, Gurny R, Biocompatibility of a new semisolid bioerodible poly(ortho ester) intended for the ocular delivery of 5-fluorouracil, J. Biomed. Mater. Res 28 (9) (1994) 1037–1046. [PubMed: 7814431]

[45]. Shive MS, Anderson JM, Biodegradation and biocompatibility of PLA and PLGA microspheres, Adv. Drug Deliv. Rev 28 (1) (1997) 5–24. [PubMed: 10837562]

[46]. Kohane DS, Langer R, Biocompatibility and drug delivery systems, Chem. Sci 1 (4) (2010) 441–446.

[47]. Li Y, Owens GE, Kohane DS, Materials for controlled release of local anesthetics, ChemMedChem 18 (11) (2023) e202300009. [PubMed: 37070644]

[48]. Hogan Q, Dotson R, Erickson S, Kettler R, Hogan K, Local anesthetic myotoxicity: a case and review, Anesthesiology 80 (4) (1994) 942–947. [PubMed: 8024149]

[49]. Bainton CR, Strichartz GR, Concentration dependence of lidocaine-induced irreversible conduction loss in frog nerve, Anesthesiology 81 (3) (1994) 657–667. [PubMed: 8092513]

[50]. Barnet CS, Louis DN, Kohane DS, Tissue injury from tricyclic antidepressants used as local anesthetics, Anesth. Analg 101 (6) (2005) 1838–1843. [PubMed: 16301270]

[51]. Shichor I, Shomron N, Lawlor MW, Bae SA, Zoldan J, Langer R, Kohane DS, Toxicogenomic analysis of a sustained release local anesthetic delivery system, Biomaterials 33 (13) (2012) 3586–3593. [PubMed: 22341215]

[52]. Drager C, Benziger D, Gao F, Berde CB, Prolonged intercostal nerve blockade in sheep using controlled-release of bupivacaine and dexamethasone from polymer microspheres, Anesthesiology 89 (4) (1998) 969–979. [PubMed: 9778015]

[53]. McAuley JH, Rothwell JC, Marsden CD, Frequency peaks of tremor, muscle vibration and electromyographic activity at 10 Hz, 20 Hz and 40 Hz during human finger muscle contraction may reflect rhythmicities of central neural firing, Exp. Brain Res 114 (3) (1997) 525–541. [PubMed: 9187289]

[54]. Li Y, Ji T, Torre M, Shao R, Zheng Y, Wang D, Li X, Liu A, Zhang W, Deng X, Yan R, Kohane DS, Aromatized liposomes for sustained drug delivery, Nat. Commun 14 (1) (2023) 6659. [PubMed: 37863880]

[55]. Bavli Y, Rabie M, Fellig Y, Nevo Y, Barenholz Y, Liposomal bupivacaine (Bupigel) demonstrates minimal local nerve toxicity in a rabbit functional model, Pharmaceutics 13 (2) (2021).

[56]. Weldon C, Ji T, Nguyen MT, Rwei A, Wang W, Hao Y, Zhao C, Mehta M, Wang BY, Tsui J, Marini RP, Kohane DS, Nanoscale bupivacaine formulations to enhance the duration and safety of Intravenous regional anesthesia, ACS Nano 13 (1) (2019) 18–25. [PubMed: 30351910]

[57]. Orkoula MG, Kontoyannis CG, Markopoulou CK, Koundourellis JE, Quantitative analysis of liquid formulations using FT-Raman spectroscopy and HPLC the case of diphenhydramine hydrochloride in Benadryl, J. Pharm. Biomed. Anal 41 (4) (2006) 1406–1411. [PubMed: 16621405]

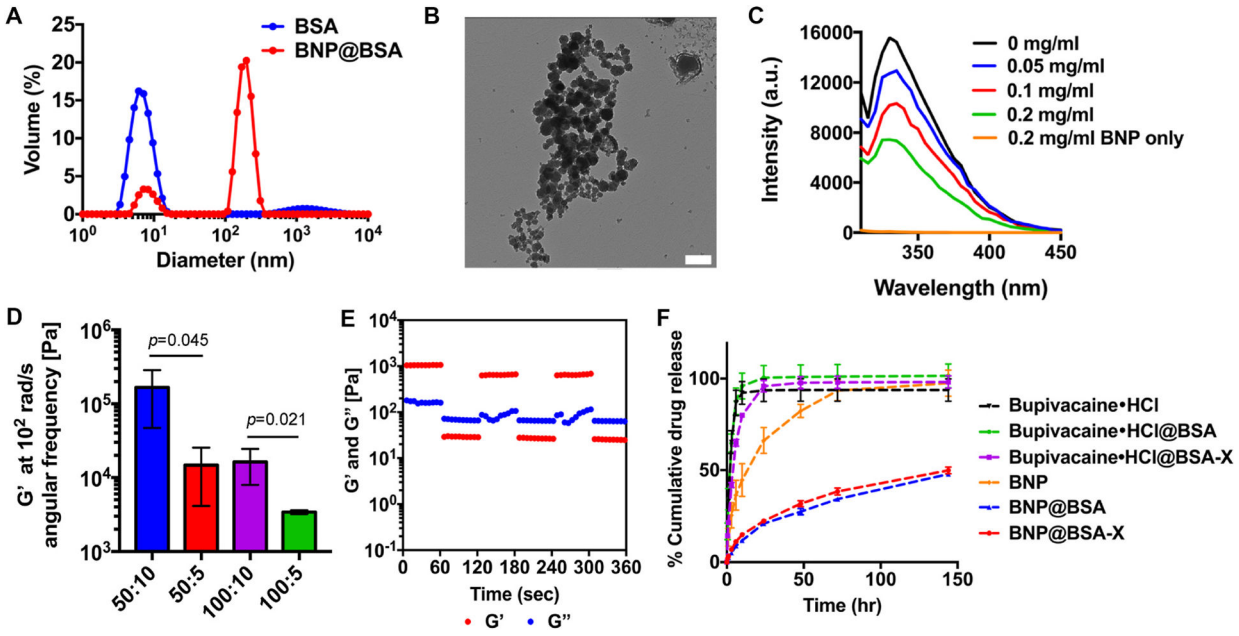

Fig. 1.

Characterization of BNP@BSA-X. (A) Size distribution by volume percent of BSA and BNP@BSA measured by dynamic light scattering (DLS). (B) Transmission electron micrograph (TEM) of BNP@BSA. Scale bar: 100 nm. (C) Fluorescent emission spectra of BSA solution with different concentrations of BNP using fluorescence spectroscopy. Excitation: 280 nm, Emission: 310–450 nm. (D) Comparison of the storage moduli (G′) at an angular frequency of 10^2 rad/s for BNP@BSA-X with varying concentrations of BSA and GA. Data are means ± SD (n = 4). (E) Mechanical properties of BNP@BSA-X (50:5; 50 mg/ml of BSA and 5 mg/ml of GA) determined by rheometry in response to repeated shear strain. Strain was applied at 0.1 % for 60 s (white regions), followed by 500 % for 60 s (blue regions). This was repeated three times. (F) Cumulative bupivacaine release (as a percentage of the total amount loaded) from formulations. Data are means ± SD (n = 4).

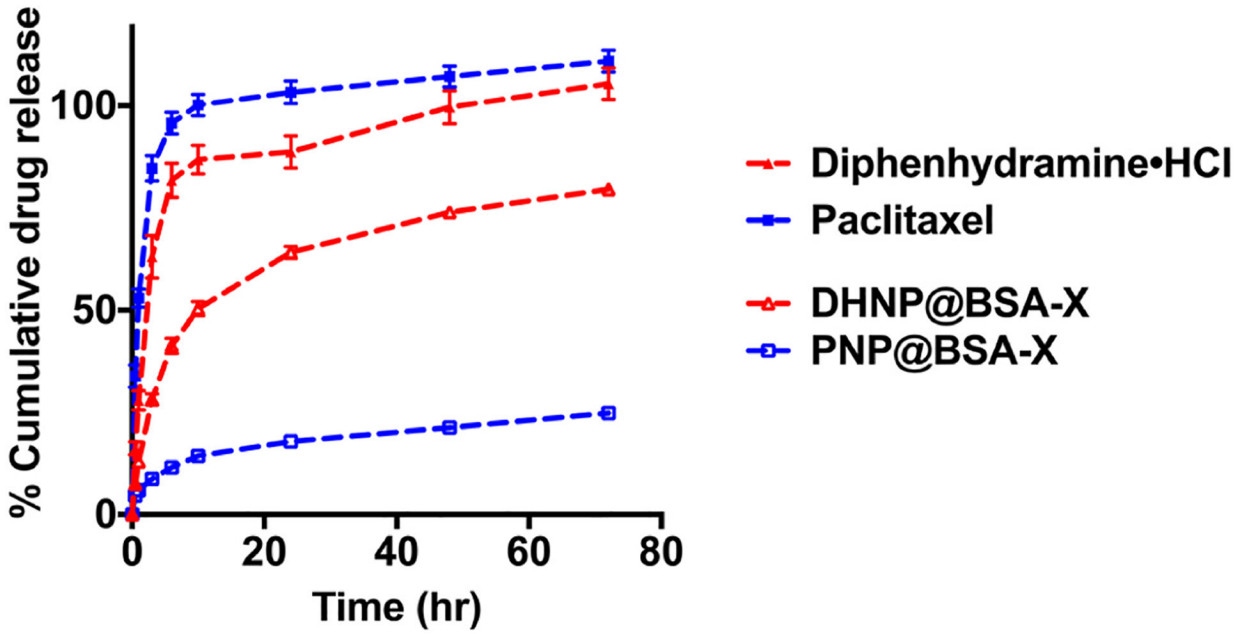

Fig. 2.

Cumulative drug release (as a percentage of the total amount loaded) from free drugs (diphenhydramine•HCl and paclitaxel) and their corresponding nanoparticles in BSA-X. Data are means ± SD ($n = 4$). p-values compare groups at 24 h.

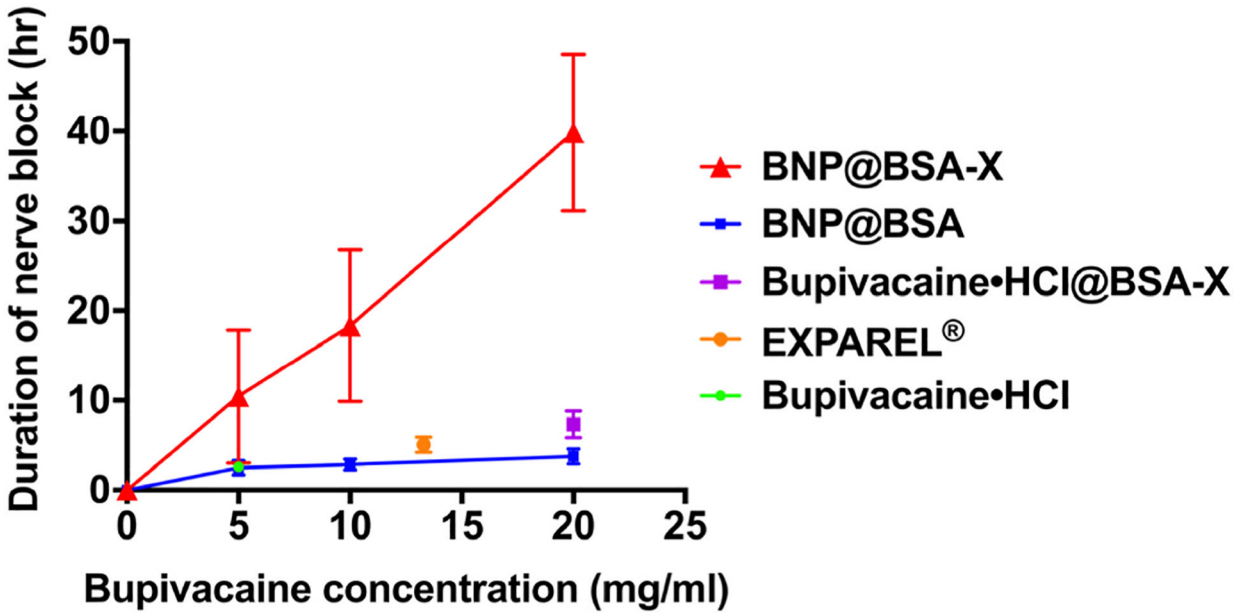

Fig. 3.

Sciatic nerve blockade. Sensory block duration from bupivacaine•HCl (5 mg/ml), and various concentrations of bupivacaine nanoparticles in uncrosslinked and crosslinked BSA (BNP@BSA and BNP@BSA-X, respectively). Also shown are the durations of block from, bupivacaine•HCl@BSA-X (20 mg/ml) and EXPAREL® (13.3 mg/ml). Data are means ± SD (n = 4–9). p-values compare groups at 20 mg/ml of bupivacaine.

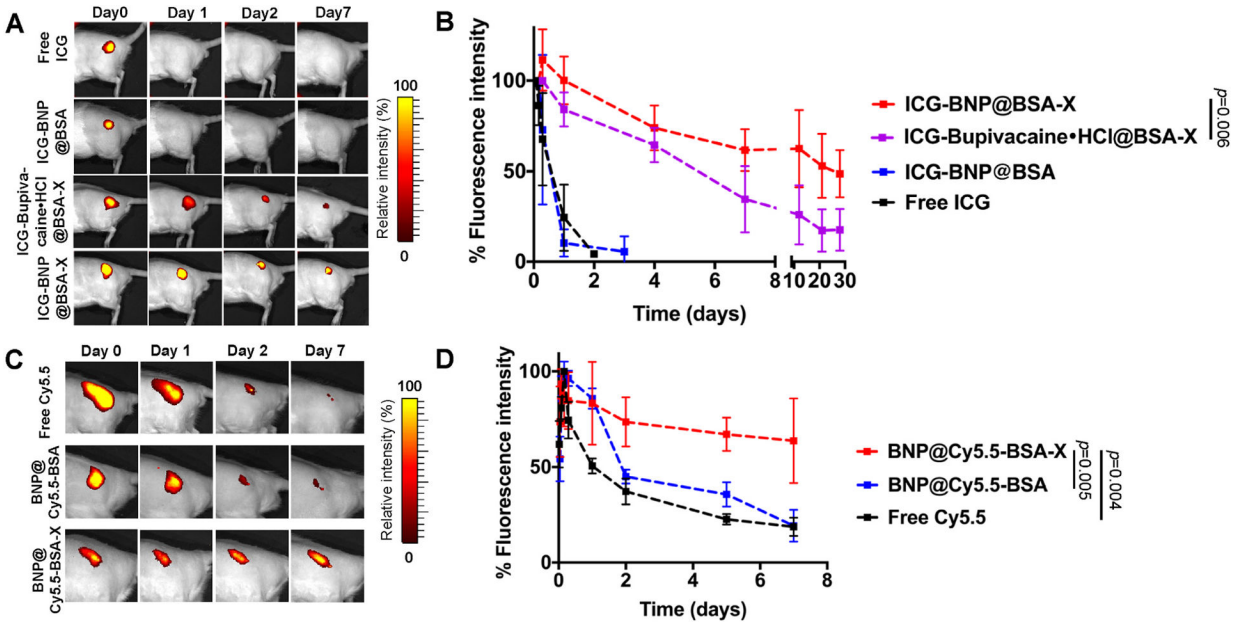

Fig. 4.

Tissue retention of fluorescently labeled formulations injected at the sciatic nerve, detected by IVIS. (A) Representative time courses of retention of ICG-containing formulations. (B) Quantification of the fluorescence intensity over time, derived from data such as those in (A). Data are means ± SD (n = 4). p-values compare groups at 28 days. (C) Representative time courses of retention of Cy5.5-containing formulations. (D) Quantification of the fluorescence intensity over time, derived from data such as those in (C). Bupivacaine concentration was 20 mg/ml. Data are means ± SD (n = 4). p-values compare groups at 7 days.

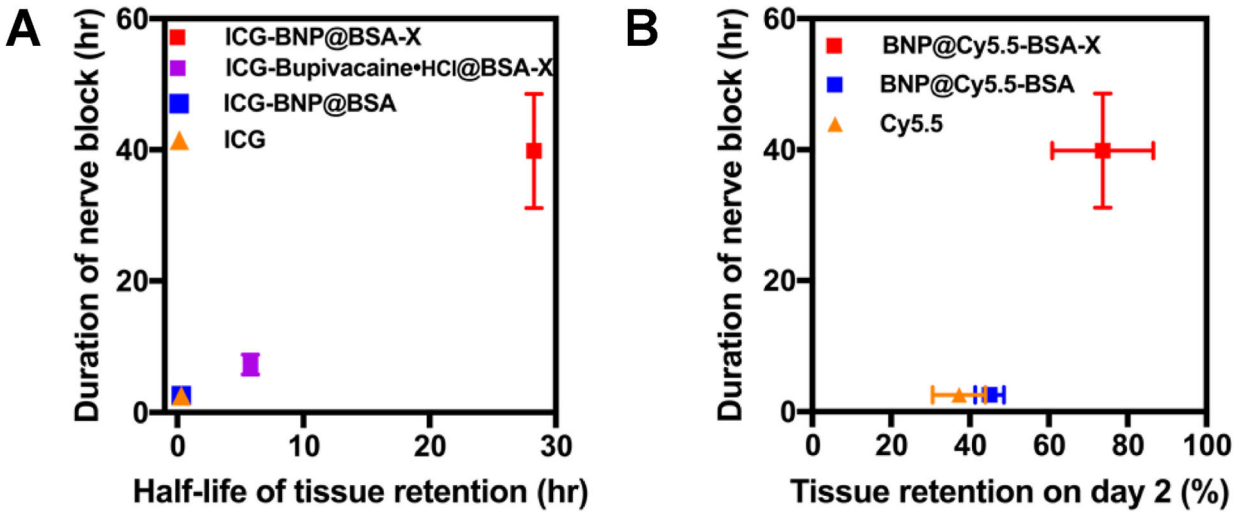

Fig. 5.

Comparison of tissue retention and the duration of sensory nerve block for different formulations. Correlation of duration of sensory nerve block with (A) the half-life of tissue retention of ICG and (B) tissue retention of Cy5.5 on day 2.

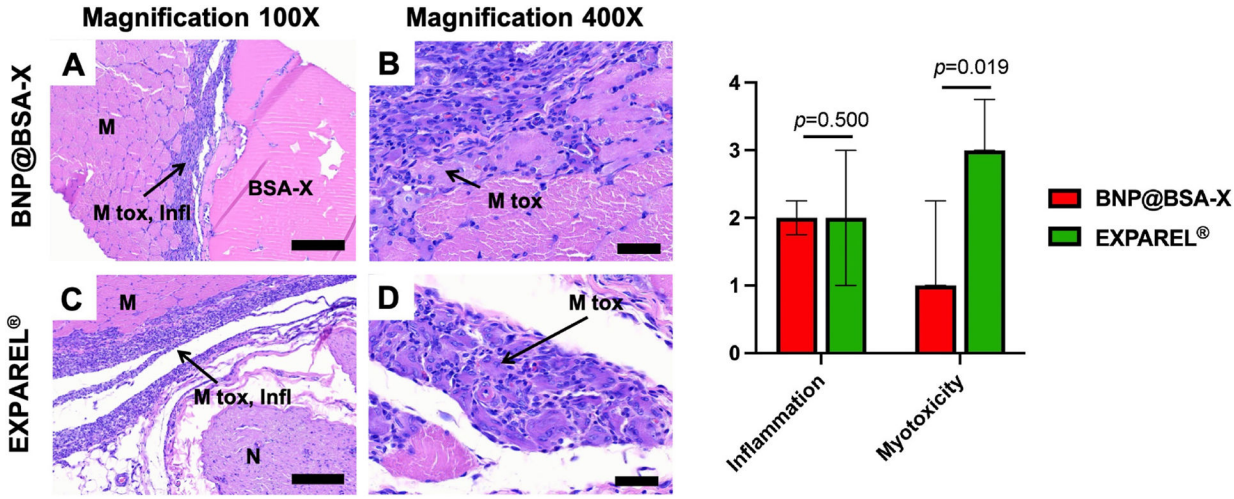

Fig. 6.

Representative hematoxylin-eosin stained sections of muscle and nerve 4 days after injection. (A and B) BNP@BSA-X with 20 mg/ml bupivacaine. (C and D) EXPAREL®. Scale bar: 200 μm (magnification 100×, panels A and C), 40 μm (magnification 400×, panels B and D). M: muscle, Mtox: myotoxicity, N: nerve, Infl: inflammation, BSA-X: crosslinked BSA. (E) Scores for tissue reaction on day 4. Data are medians with interquartile ranges (n = 4–6). *p* values are calculated from Mann-Whitney *U* test.

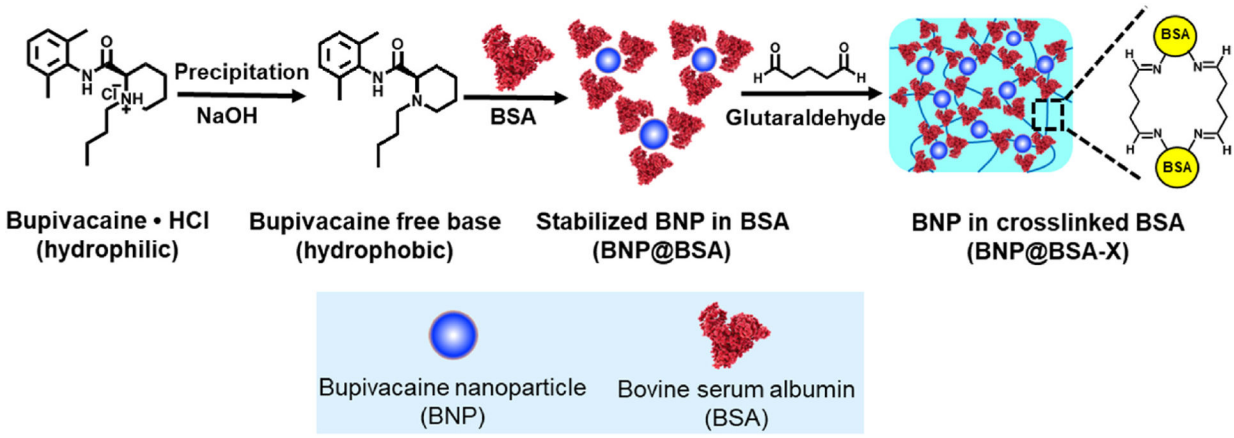

Scheme 1.

Synthetic scheme of BNP@BSA-X, a glutaraldehyde-crosslinked bovine serum albumin hydrogel (BSA-X) containing bupivacaine free base nanoparticles (BNPs).